Available online at www.sciencedirect.com
ScienceDirect
Experimental Neurology 201 (2006) 416–427
Experimental Neurology
www.elsevier.com/locate/yexnr

Degeneration and proliferation of astrocytes in the mouse dentate gyrus after pilocarpine-induced status epilepticus

Karin Borges [a,d,*], Dayna McDermott [a,c], Hasan Irier [a], Yoland Smith [b,c], Raymond Dingledine [a]

[a] Department of Pharmacology, Emory University, Atlanta, GA 30322, USA
[b] Yerkes National Primate Research Center, Emory University, Atlanta, GA 30322, USA
[c] Department of Neurology, Emory University, Atlanta, GA 30322, USA
[d] Department of Pharmaceutical Sciences, Texas Tech University, Amarillo, TX 79106, USA

Received 14 October 2005; revised 14 April 2006; accepted 28 April 2006
Available online 21 June 2006

Abstract

Astrocytes are relatively resistant to injury compared to neurons and oligodendrocytes. Here, we report transient region-specific loss of astrocytes in mice early after pilocarpine-induced status epilepticus (SE). In the dentate hilus, immunoreactivity for glial acidic fibrillary protein (GFAP) was decreased, and the number of healthy appearing GFAP- or S100β-positive cells was significantly reduced (≥65%) 1 and 3 days after pilocarpine-induced SE. Many remaining GFAP-positive cells were shrunken, and 1 day after SE electron microscopy revealed numerous electron-dense degenerating astrocyte processes and degenerating glial somata in the hilus. Degeneration of GFAP-expressing cells may be linked to hilar neuronal death, because we did not observe loss of astrocytes after kainate-induced SE, after which hilar neurons remained intact. Ten days after SE, hilar GFAP immunoreactivity had returned, partially from GFAP-positive cells in the hilus. Unlike control mice, many GFAP-positive hilar processes originated from cell bodies located in the subgranular zone (SGZ). To investigate whether proliferation contributes to hilar repopulation, we injected 5-bromo-2′-deoxyuridine (BrdU) 3 days after SE. Five hours later and up to 31 days after SE, many BrdU/GFAP colabeled cells were found in the hilus and the SGZ, some with hilar processes, indicating that proliferation in both areas contributes to generation of hilar astrocytes and astrocyte processes. In contrast to pilocarpine-induced SE in mice, astrocyte degeneration was not found after pilocarpine-induced SE in rats. These findings demonstrate astrocyte degeneration in the mouse dentate hilus specifically in the mouse pilocarpine epilepsy model, followed by astrogenesis leading to hilar repopulation.

Keywords: Stem cell; Seizure; Hilus; Kainate; Glial fibrillary acidic protein; Adult progenitor cell; Mouse strain

Introduction

Astrocytes play many important roles in glutamate and potassium uptake, production of growth factors, cytokines and extracellular matrix proteins, in both the healthy and injured central nervous system (Kettenmann and Ransom, 2004). Within the last decade, it has become increasingly clear that astrocytes and neurons communicate chemically (e.g., reviewed in Newman, 2003). A recent study suggests that calcium waves in astrocytes can trigger astrocytic glutamate release inducing paroxysmal depolarization shifts (Tian et al., 2005), abnormal prolonged depolarizations that are observed during interictal activity. Gliosis following injury or status epilepticus (SE) is marked by the overexpression of glial fibrillary acidic protein (GFAP) by reactive astrocytes (Eng et al., 1992). Compared to neurons and oligodendrocytes, which are both very vulnerable to glutamate-mediated death occurring during ischemia (Petito et al., 1998), astrocytes are relatively resistant to injury. Astrocytes can, however, be selectively damaged by injection of "glial-toxic" drugs, including 3-chloropropanediol (Willis et al., 2004), the aconitase inhibitor fluorocitrate (Paulsen et al., 1987), or 6-aminonicotinamide (see Krum, 1994 and references therein). Moreover, apoptotic astrocytes have been found in the early

* Corresponding author. Department of Pharmaceutical Sciences, Texas Tech University School of Pharmacy, 1300 S Coulter Dr., Amarillo, TX 79106, USA. Fax: +1 806 356 4034.
E-mail address: karin.borges@ttuhsc.edu (K. Borges).

0014-4886/$ - see front matter © 2006 Elsevier Inc. All rights reserved.
doi:10.1016/j.expneurol.2006.04.031

stages of Huntington's disease (Thomas et al., 1995). During development and throughout adult life, neural stem cells in the subgranular zone (SGZ) proliferate and generate neurons (reviewed in Gage et al., 1998; Parent, 2003; Kempermann et al., 2004; Lie et al., 2004) and to a lesser extent astrocytes (Palmer et al., 2000; Kempermann and Gage, 2002; Steiner et al., 2004). Lineage tracing in vitro and in vivo using GFAP-promoter controlled expression of green fluorescent protein suggests that adult neural precursor cells express GFAP and at early stages have the morphology of radial glia (e.g., Seri et al., 2001, 2004; Garcia et al., 2004). After seizures, proliferation of subgranular adult stem cells fuels neurogenesis (Bengzon et al., 1997; Parent et al., 1997; Scott et al., 2000; Ferland et al., 2002; Huttmann et al., 2003), but, to our knowledge, whether astrogenesis is also enhanced after seizures is unknown.

Seizures are well-known to induce overexpression of GFAP in astrocytes (gliosis); and in some models, proliferation and swelling of astrocytes have been described (Nadler et al., 1980; Niquet et al., 1994, Nitecka et al., 1984). Only a few studies report evidence for astrocyte degeneration after SE in animal models (Motte et al., 1998; Revuelta et al., 2005) and potentially in humans (Gurnett et al., 2003).

While studying the neuropathology of the mouse pilocarpine model, in which mice develop spontaneous recurrent seizures, we found reactive astrocytes 10 to 31 days after SE in areas showing neuronal damage, including the dentate hilus (Borges et al., 2003a). We now provide evidence at the light and electron microscopic levels that many astrocytes in the mouse hilus degenerate 1 to 3 days after SE. We studied the mechanism of hilar astrocyte repopulation between 3 and 31 days. Labeling with 5-bromo-2′-deoxyuridine (BrdU) shows enhanced astrocyte proliferation in the hilus and SGZ 3 to 7 days after SE. Moreover, 1 week after SE, hilar GFAP- and S100β-containing processes often originate from cell bodies in or near the SGZ, some of which are BrdU-labeled, suggesting that astrogenesis in the SGZ contributes to the subsequent repopulation of the hilus with astrocytes. Some of the results have been presented in abstract form (Borges et al., 2003b).

Materials and methods

Pilocarpine injections were performed as described in outbred CF1 mice (Borges et al., 2003a, 2004). Briefly, mice were injected with methylscopolamine and terbutaline (2 mg/kg each i.p. in 0.9% NaCl) 15–30 min prior to pilocarpine (275–310 mg/kg, i.p.) to minimize peripheral side effects. Thirty percent of CF1 injected mice experienced behavioral SE for about 5 h as defined by continuous behavioral seizure activity consisting of mainly whole body clonic seizures (see Borges et al., 2003a for a more detailed description of seizure behavior including a modified Racine scale). Mice showing behavioral seizure activity for less than 1 h were used as a "no SE control" group. Control mice received terbutaline and methylscopolamine, but no pilocarpine.

We also induced pilocarpine-induced seizures in two inbred 129 substrains from two different sources (wild-type counterparts of osteopontin-lacking mice). 129 mice, derived from AB2.1 mouse stem cells were obtained from Dr. Susan Rittling (Rittling et al., 1998) termed here 129(AB2.1) and 129/Sv (Taconic, Hudson, NY) mice were obtained from Dr. Lucy Liaw (Liaw et al., 1998) termed here 129/SvTac. Eleven 129(AB2.1) mice (19–31 g) were injected with 270–310 mg/kg pilocarpine (i.p.) inducing SE in ten mice with seven mice surviving SE. One mouse did not experience SE. Five mice did not experience SE after they received 260 mg/kg pilocarpine (i.p.), and they were used as a "no SE control" group. Eight 129/SvTac mice were injected with 240 mg/kg pilocarpine (i.p.), leading to SE in three mice, no SE in four mice ("no SE control" group) and one death.

Sections from CF1 mice with SE induced by repeated kainate injection were used from the previous study (Borges et al., 2004). Briefly, kainate (5–20 mg/kg, i.p. in phosphate-buffered salt solution) was injected every 30 min until SE was reached. After 4 to 5 h of behavioral SE, seizures were terminated by injection of 25 mg/kg pentobarbital (i.p.). Three mice were videotaped for potential spontaneous behavioral seizures between days 14 and 35 for up to 27 h total.

Sprague Dawley rats (150–220 g, Charles River) were injected with 127 mg/kg lithium chloride 19–24 h before injection with methylscopolamine and terbutaline (2 mg/kg each i.p in 0.9% NaCl) followed 20 min. later by pilocarpine (30 mg/kg, i.p., Clifford et al., 1987). In some rats, lithium was not used and 340 mg/kg pilocarpine was given. SE was terminated after 90 min of SE in the lithium/pilocarpine-injected rats, or after 2.5 h in the pilocarpine-injected rats, by injection of 20–25 mg/kg pentobarbital (i.p.). After SE, all animals were fed moistened rodent chow and were injected with 5% dextrose in lactate Ringer's solution as needed. Control rats were given saline instead of pilocarpine.

To label proliferating cells in the hilus, a single injection of 5-bromo-2′-deoxyuridine (BrdU, 100 mg/kg, i.p., Sigma) was made 3 days after SE. Mice were sacrificed at different time points after BrdU injection, namely 5 h (four mice 3 days after SE and three control mice), 4 days (three control mice and five mice 7 days after SE), 7 days (three mice 10 days after SE) and 28 days (three mice 31 days after SE). All experiments were approved by the Institutional Animal Care and Use Committee (IACUC) of Emory University and conducted in accordance with its guidelines. Every effort was made to minimize animal suffering.

After decapitation under flurothane anesthesia, brains were removed, fixed in 4% paraformaldehyde and embedded in paraffin blocks. Eight-micrometer-thick brain sections were deparaffinized, blocked with normal serum and then incubated with primary antibodies directed against the astrocyte marker GFAP (rabbit anti-cow GFAP, Dako Inc., Carpintaria, CA, 1:500), followed by species-specific biotinylated secondary antibody, avidin–biotin-peroxidase complex according to the manufacturer (Vector Laboratories, Burlingame, CA) and color development with 0.6 mg/ml 3,3′-diaminobenzidine (DAB)/0.03% hydrogen peroxide and hematoxylin counterstaining.

For BrdU double-labeling with cell-specific antibodies, we used fluorescent immunohistochemistry after microwaving sections in 1 mM sodium citrate buffer, pH 6.0. Sections were incubated with the monoclonal mouse anti-BrdU antibodies (BD Pharmingen, San Diego, CA; 1:100) together with rabbit anti-GFAP (Dako, 1:500), rabbit anti-S100β (Swant, Bellinzona, Switzerland, 1:500) or goat–anti-doublecortin antibodies (C-18, 1:100, Santa Cruz Biotechnologies Inc., Santa Cruz, CA). For

visualization, CY3-conjugated goat anti-rabbit antibodies (Dako, 1:400 for visualization of GFAP) together with biotinylated horse anti-mouse antibodies followed by streptavidin-conjugated CY2 (Dako, 1:200, for BrdU) were used. Alternatively, we used FITC-labeled donkey anti-mouse antibodies (for visualization of BrdU) together with biotinylated goat anti-rabbit antibodies (for S100β) or biotinylated rabbit anti-goat antibodies followed by streptavidin-conjugated CY3 (1:200, for doublecortin). All biotinylated antibodies were from Vector Labs and used at a 1:200 dilution. For BrdU double-labeling with the microglial marker *Griffonia simplicifolia* isolectin B_4, sections were first pretreated for 10 min with pepsin (Biomeda Corp., Foster City, CA) and then microwaved as described above. BrdU antibodies were incubated together with biotinylated *G. simplicifolia* isolectin B_4 (Sigma, 1:40) overnight and visualized with CY2-labeled donkey anti-mouse antibodies (1:100, for BrdU) together with streptavidin-conjugated CY3 (1:200, for lectin). In all fluorescent stainings, nuclei were stained with Hoechst 33258 (Molecular Probes, Eugene, OR). All other fluorescent reagents were from Jackson ImmunoResearch Laboratories, Inc. (West Grove, PA).

Sections between −2.1 and −2.5 mm to bregma (corresponding to the dorsal hippocampus, Hof et al., 2000) were used for counting. Cells were counted within the total area of the hilus and the dentate molecular layer (for definition of areas, see Fig. 2A). The hilus was defined as the area between the dentate granule cells and a line perpendicular to the tip of the CA3c pyramidal cell layer. The SGZ, about one cell diameter on the hilar border area along the dentate granule cell layer, was not included when counting hilar cells. The area outside the granule cell layer and bordered by the hippocampal fissure was defined as the molecular layer.

Non-fluorescent sections were counted by direct microscopic examination. Hilar neurons were identified by blue hematoxylin staining of their large somata and several dark nucleoli. The numbers of GFAP-positive cells with light blue hematoxylin-stained round cell bodies (defined as "healthy") were counted for each mouse in at least two randomly chosen sections. For fluorescent double stainings of BrdU with GFAP or doublecortin, we used a Zeiss LSM size 510 confocal microscope with argon (488-nm excitation) and Helium/Neon (543-nm excitation) lasers and two-photon excitation of Hoechst dye using a titanium sapphire (755nm) laser. Zeiss AIM software was used for imaging and analysis through the *z*-axis of each 8-μm section in 0.4–1.5 μm increments. GFAP/BrdU stainings were imaged in at least four hilar sections of each mouse using a 40 ×, 63 × or 100 × oil immersion objective. BrdU-positive nuclei surrounded or adjacent to GFAP immunoreactivity in several z-sections were counted as GFAP-positive. Doublecortin/BrdU-double-stainings were first selected by light microscopy and then imaged for typical double-stained cells and typical BrdU-positive, doublecortin-negative cells. In confocal sections, "healthy" and shrunken nuclei could not be distinguished. Moreover, cell counting was semiquantitative because sections were only eight microns thick. For fluorescent double-stainings of BrdU with S100β or lectin, images of BrdU, S100β or lectin and nuclear labelings were taken using a Leitz fluorescent microscope with 20 × and 40 × objectives and a Leica digital camera and were overlayed in Photoshop. S100β/BrdU-double-stainings were counted on the computer screen (1–3 sections per mouse, $n = 5$ mice). Cell counts were averaged for each mouse and were compared among treatment groups using one-way ANOVAs followed by a Bonferroni post hoc test with selected pairs or a Dunnett's multiple comparison test relative to control; $^{*}P < 0.05$, $^{**}P < 0.01$, $^{***}P < 0.001$. The mean and standard error (SEM) across a group of mice is given.

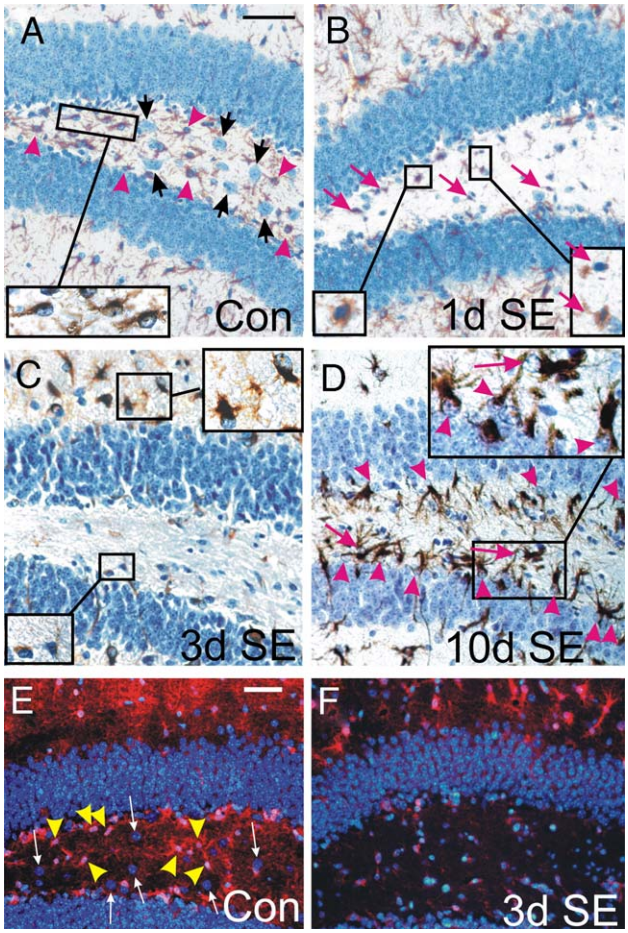

Fig. 1. Immunoreactivity for hilar GFAP (A–D) and S100β (E, F) is transiently reduced in CF1 mice after pilocarpine-induced SE. Dentate gyrus paraffin sections of a control mouse (A) and mice 1, 3 and 10 days after SE (B–D, as indicated in the lower right corner) were immunostained for GFAP (brown) and counterstained with hematoxylin (blue). (A) Black arrows point to hilar neurons identified by their size and nucleoli, and pink arrowheads point to representative astrocytes containing oval or round light blue nuclei, defined as healthy (enlarged in inset). (B, C) One and three days after pilocarpine-induced SE, there is loss of GFAP immunoreactivity in the hilus. The remaining GFAP-expressing cells mainly contain dark and shrunken nuclei (pyknotic, pink arrows, enlarged in bottom insets) and only short GFAP-positive processes. GFAP-positive cells in the dentate molecular layer were healthy and overexpressed GFAP 3 days after SE (C, upper inset). (D) Ten days after SE, GFAP-labeled reactive astrocytes with healthy round or oval and light nuclei had reappeared in the hilus (arrows) and mainly in or near the SGZ with processes extending into the hilus (pink arrowheads, inset). (E, F) Immunostaining for S100β (red) in a control mouse (E) and a mouse 3 days after SE (F) shows loss of S100β immunoreactivity and S100β-positive cells in the hilus (yellow arrowheads). In the dentate molecular layer S100β expression is upregulated in the proximal processes of reactive astrocytes. Nuclei are stained with Hoechst 33258 (blue). Note that S100β is expressed in the nucleus, therefore S100β-positive nuclei appear purple. Hilar neurons identified by their larger size are indicated by white arrows. The bars in panel A (valid for B–D) and E (valid for F) represent 50 μm. (For interpretation of the references to colour in this figure legend, the reader is referred to the web version of this article.)

For electron microscopy, 1 day after SE, mice were anesthetized with an overdose of ketamine (75 mg/kg) and medetomidine (Dormitor, 0.5 mg/kg) and perfused with cold Ringer solution followed by 250 ml of fixative containing 4% paraformaldehyde and 0.1% glutaraldehyde in 0.1 M phosphate buffer pH 7.4. Brains were then cut into 60-μm-thick sections with a vibratome. Sections were post-fixed in 1% osmium tetroxide, dehydrated in a graded series of alcohol/propylene oxide and embedded in resin (Durcupan, Fluka) on microscope slides. After resin hardening at 60°C for 48 h, blocks of tissue from the dentate gyrus in mice were glued onto resin blocks. Ultrathin sections were cut on an ultramicrotome, collected on copper single slots grids, stained with lead citrate and examined with an electron microscope (Zeiss, EM 10C). The ultrastructural features used to categorize elements in this material were those described in Peters et al. (1991).

Results

Astrocytes degenerate in the mouse dentate hilus 1 to 3 days after pilocarpine-induced SE

GFAP immunostaining of paraffin sections at different times after pilocarpine-induced SE (Figs. 1A–D) revealed loss of GFAP labeling specifically in the hilus 1 to 3 days after SE in ten of eleven mice (Figs. 1A–C). Only one out of five mice sacrificed 1 day after SE showed abundant GFAP labeling similar to control mice. In contrast GFAP expression in astrocytes in the dentate molecular layer appeared unchanged or slightly upregulated. Loss of hilar GFAP immunoreactivity was transient, because 10 days after pilocarpine-induced SE the hilus contained many GFAP-overexpressing processes and cells (Fig. 1D). One and three days after SE, we observed that hematoxylin-stained nuclei in the hilus were often dark and shrunken, typical for pyknotic cells, and were associated with short GFAP-expressing processes, indicating that hilar astrocytes may be degenerating (Figs. 1B, C, bottom insets). In contrast, in control mice most GFAP-expressing processes were long (> 5 μm) and were associated with round or bean-shaped, light blue stained somata, which were defined as "healthy" (Fig. 1A, inset). In control mice, in sections between −2.1 and −2.5 mm to bregma (corresponding to the dorsal hippocampus, Hof et al., 2000), 21.7 ± 1.9 hematoxylin-stained healthy nuclei associated with GFAP immunoreactivity were found in the hilus per eight μm section (mean ± SEM, n = 5 mice). One and three days after SE, only 7.7 ± 2.2 (n = 5) and 8.9 ± 3.1 (n = 4) GFAP-positive cells were found, representing a 59–65% loss of healthy hilar GFAP-positive cells (Fig. 2B squares, $P < 0.01$). Mice that had received pilocarpine but did not experience SE, showed no loss of hilar astrocytes 3 days later (22.3 ± 0.5 hilar GFAP-positive cells, n = 4). This indicates that pilocarpine-induced SE, but not the drug itself, leads to loss of GFAP-staining. Similarly, immunoreactivity for the astrocyte marker S100β was lost in the hilus; on average 69% of hilar S100β-positive cells were lost 3 days after SE (Figs. 1E, F, yellow arrowheads, n = 4 mice). In contrast, in the dentate molecular layer the number of GFAP-expressing astrocytes increased slightly but not significantly 1 to 3 days after SE (Fig. 1C upper inset, Fig. 2B triangles), indicating that astrocyte loss is region-specific in the dentate gyrus. Moreover, dentate molecular

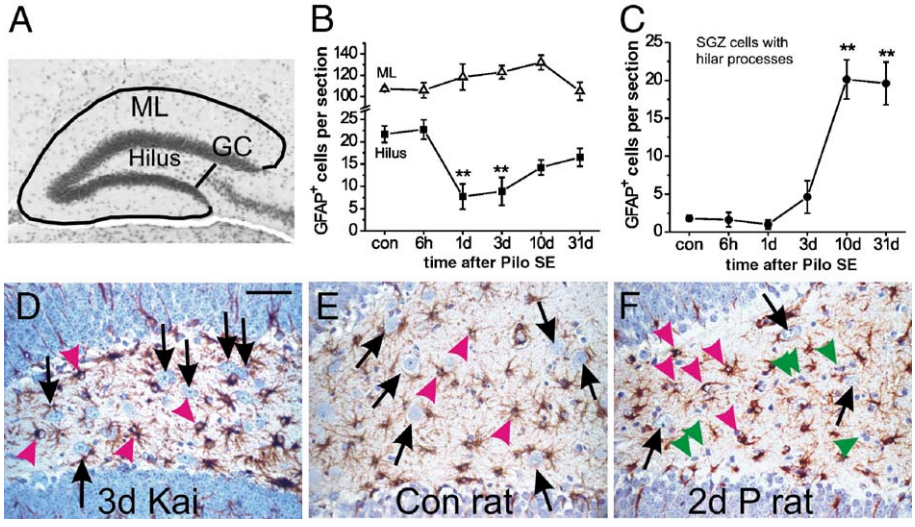

Fig. 2. Selective astrocyte death in the dentate hilus after pilocarpine-induced SE is dependent on species and method to induce SE. (A) The micrograph shows a typical dorsal dentate gyrus section with the sampled areas outlined. The hilar area is between the two blades containing the dentate granule cells and the black line perpendicular to the end of the CA3 pyramidal cell layer. The molecular layer (ML) is found outside the granule cell layer (GC) and bordered by the black lines. The average cell numbers and standard error of healthy GFAP-positive cells per 8 μm dorsal hippocampal section are shown at different times after pilocarpine-induced SE (n = 4 – 5 CF1 mice) for the dentate molecular layer (B, triangles), the hilus (B, squares) and subgranular astrocytes that show hilar processes (C). The number of healthy GFAP-expressing cells significantly declined 1 and 3 days after SE in the hilus, but not the dentate molecular layer (one-way ANOVA followed by a post hoc Dunnett test). The number of subgranular cells with hilar processes significantly increased ten and 31 days after SE (one-way ANOVA followed by a post hoc Dunnett test). All comparisons are relative to control mice. $^{**}P < 0.01$. (D–F) Representative GFAP immunostainings (brown) of the hilus are shown from a CF1 mouse 3 days after about 4 h SE induced by repeated kainate injections (D), a control rat (E) and a rat 2 days after 2.5 h SE induced by pilocarpine (F). Note that GFAP-expressing cells appear healthy (pink arrowheads) in all three sections. Hilar neurons (black arrows) are reduced in number after SE in the rat (F), but not in the mouse after kainate-induced SE. Some shrunken GFAP-negative cells, most likely dying neurons, are pointed out by green arrowheads. Sections are counterstained with hematoxylin and the scale bar is 50 μm. (For interpretation of the references to colour in this figure legend, the reader is referred to the web version of this article.)

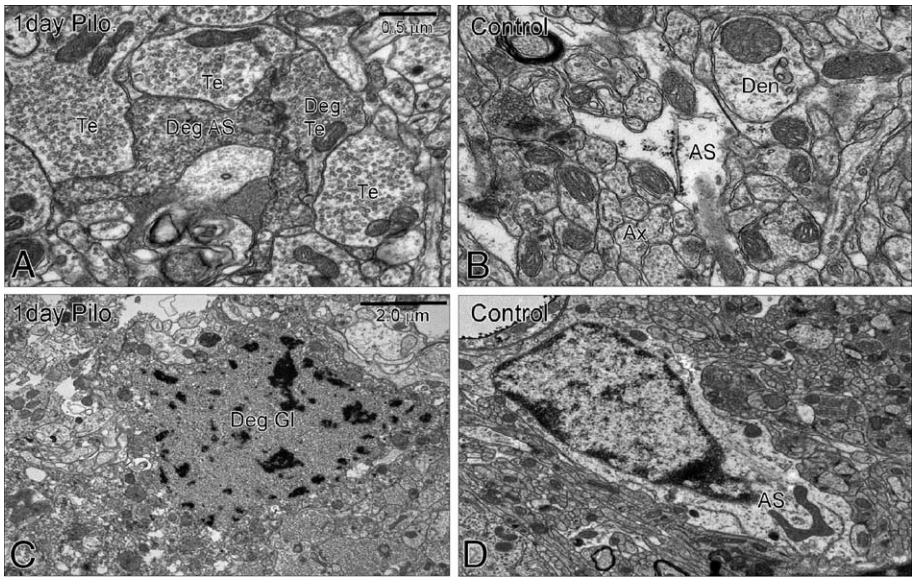

Fig. 3. Electron microscopy of the hilus of a CF1 mouse 1 day after pilocarpine-induced SE (A, C) and of a control CF1 mouse (B, D). (A) One day after SE astrocyte processes are electron dense, indicating degeneration of astrocyte processes (Deg AS). (C) Small cells were found with atypical chromatin distribution and missing nuclear membrane consistent with degenerating glia (Deg GL). In a control mouse, astrocyte processes appear light (AS in B) and the nuclear membrane is intact (D) consistent with healthy astrocyte morphology (AS). Synaptic terminals that appear healthy (Te) or electron-dense, i.e., degenerating (Deg Te), are labeled. Den, dendrite; Ax, axon.

astrocytes appeared reactive with overexpression of GFAP and S100β, and a stouter morphology (Fig. 1C upper insets and Fig. 1F). Six hours after SE, many hilar neurons are lost (Borges et al., 2003a), but GFAP-positive cells contained healthy nuclei and the number of hilar healthy GFAP-positive cells was similar to control mice (Fig. 2B, squares), indicating that astrocyte degeneration occurs after neuronal damage. Ten days after SE subgranular astrocytes with hilar processes were prominent (Fig. 1D, arrowheads) and their numbers remained high at 31 days (Fig. 2C, $P<0.01$).

Electron microscopy

To confirm astrocyte degeneration in the mouse hilus after pilocarpine-induced SE, we performed electron microscopy. One day after SE, many electron-dense, degenerating astrocyte processes (Fig. 3A) were found in the hilus, consistent with our findings at the light microscopic level. The degenerated processes were classified as astrocytic because of their widespread distribution throughout the neuropil in close contact with neuronal elements including, cell bodies, dendrites and axon terminals, a characteristic feature of astrocytic processes (Peters et al., 1991). No other glial cells display such a pattern of distribution and form tight sheet-like plexuses of glial processes in close contact with neuronal structures. Moreover, small cell bodies with damaged nuclear membrane and atypical chromatin distribution were found in the hilus, which were classified as glial cell bodies because of their small size (Fig. 3C). No degenerated glial cell bodies were observed in the granule cell layer, indicating that shortly after pilocarpine-induced SE, astrocyte degeneration

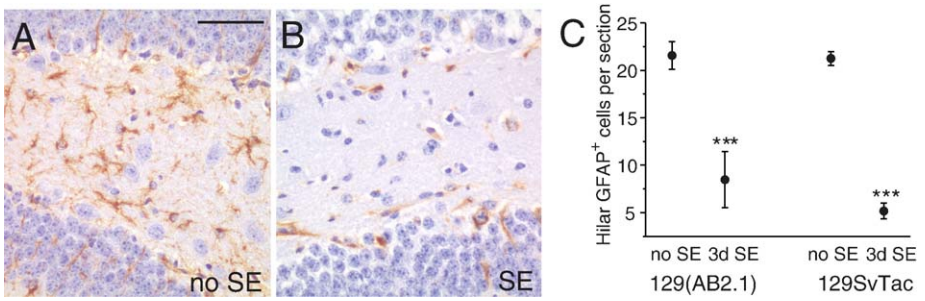

Fig. 4. Significant loss of healthy hilar GFAP-expressing astrocytes 3 days after pilocarpine-induced SE in 129 mice. (A, B) Hilar GFAP immunoreactivity (brown) in a 129(AB2.1) mouse that did not experience SE (A) and one that did (B). (C) The average number of hilar healthy GFAP-positive astrocytes per section (±SEM) is shown for 129(AB2.1) with and without SE (both $n=3$) and 129/SvTac mice (no SE: $n=4$; SE: $n=3$), showing a statistically significant loss in both substrains (two-tailed unpaired t test, ***$P<0.001$). Scale bar is 50 μm. (For interpretation of the references to colour in this figure legend, the reader is referred to the web version of this article.)

occurs specifically in the hilus. In control mice, astrocyte processes are light, and chromatin is densest close to the nuclear membrane (Figs. 3B, D).

Astrocyte loss in the 129 mouse strain and other epilepsy models

It is well-known that kainate-induced seizures induce different degrees of cell death in various mouse strains. Therefore, we evoked SE by pilocarpine injection (i.p.) in two inbred 129 substrains, 129 (AB2.1) and 129/SvTac. Loss of astrocytes in the dentate hilus was very reproducible in outbred CF1 mice and was also found in both 129 substrains (Fig. 4). The behavior and duration of seizures in these mouse strains were similar with seizures starting after about 20–45 min after pilocarpine injection and SE lasting for about 5 h. All mice mainly showed constant whole body clonic seizures with occasional tonic–clonic seizures occurring in some mice. Three days after pilocarpine-induced SE, 129(AB2.1) mice showed 40–78% loss of GFAP-positive cells in

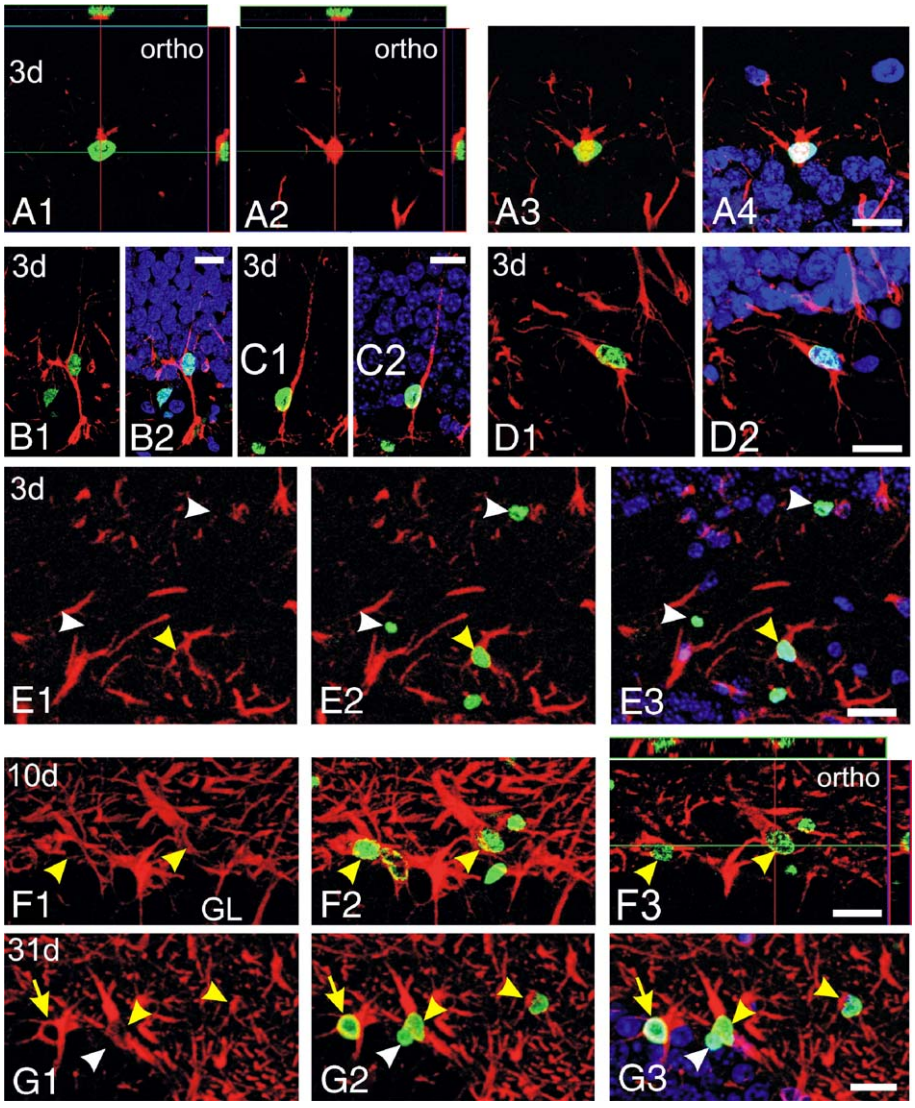

Fig. 5. Proliferation and generation of GFAP-positive astrocytes in the CF1 mouse hilus and SGZ after pilocarpine-induced SE. Confocal images of BrdU/GFAP-double-fluorescent stainings in the hilus and SGZ are shown with BrdU (green) and GFAP (red) as projections. Some panels show orthogonal slices (ortho, A1, A2, F3) with the main *xy* section in the middle, the green line indicating the position of the *xz* slice shown on the top and the red line indicating the position of the *yz* slice located on the right of each panel. Mice were injected with BrdU 3 days after SE and were analyzed after 5 h (A–E), 7 days after BrdU and 10 days after SE (F) or 28 days after BrdU and 31 days after SE (G). All panels depict BrdU and GFAP labelings, except for E1, F1 and G1 which show GFAP staining only. In some panels, Hoechst 33285 is included for orientation (panels A4, B2, C2, D2, E3, G3). Panels A–C show different BrdU/GFAP-double-labeled cell types found in the SGZ 3 days after SE: (A) a presumptive subgranular astrocyte with a horizontally aligned nucleus and (B, C) radial glia-like cells, with the cell in panel B displaying a presumptive endfoot in the hilus. Note that the BrdU-positive nucleus in panel A is only partially included in the section, but it is surrounded cytoplasmic GFAP labeling on its superior side. Hilar BrdU/GFAP-colabeled cells, presumably proliferating or injured astrocytes, are shown in panels D and E (yellow arrowhead). BrdU-positive, but GFAP-negative, cells are pointed out by white arrowheads (E). (F, G) BrdU/GFAP-double-labeled cells with astrocytic morphology were found in the hilus (yellow arrowheads) and the SGZ (yellow arrow) 10 and 31 days after SE, indicating that proliferation generated new astrocytes after pilocarpine-induced SE. A BrdU-positive/GFAP-negative cell near the subgranular layer is pointed out by a white arrowhead, demonstrating that not all BrDU-positive cells were GFAP-labeled. GL — granule cell layer. Scale bars 20 μm. (For interpretation of the references to colour in this figure legend, the reader is referred to the web version of this article.)

the hilus (61 ± 14%, $n = 3$ mice, $P < 0.001$, Figs. 4A-C) and 129/SvTac mice exhibited 69–79% loss (76 ± 4%, $n = 3$, $P < 0.001$, Fig. 4C). Similar to CF1 mice both inbred 129 mouse strains showed about 95% loss of hilar neurons 3 days after SE ($n = 3$ each) compared to the no SE control goup ($n = 3$ 129(AB2.1), $n = 4$ 129/SvTac mice). In mice with severe damage in the CA3 and CA1 pyramidal cell layers we also observed loss of GFAP immunoreactivity in the hippocampal CA1 and CA3 areas, as well as in the piriform cortex, 3 days after pilocarpine-induced SE (unpublished).

In contrast to pilocarpine-induced SE, after SE induced by repeated kainate injections we observed no reduction in the number of hilar astrocytes (22.3 ± 0.5 GFAP-positive hilar cells per section, $n = 6$; Fig. 2D). Interestingly, we were unable to detect any spontaneous behavioral seizures during 10–27 h cumulative videotapes of three mice filmed between 14 to 35 days after kainate-induced SE, in contrast to an average of one spontaneous motor seizure observed every 12.5 h after pilocarpine-induced SE (Borges et al., 2003a). Moreover, in rats hilar astrocytes appeared healthy at the light microscopic level 1 to 3 days after SE either induced by pilocarpine alone ($n = 3$, Figs. 2E, F, pink arrowheads) or by lithium/pilocarpine ($n = 10$). Cell counts after pilocarpine-induced SE in the rat (no lithium) revealed about 50% reduction in hilar neurons, but no change in astrocyte numbers (not shown).

Partial astrocyte repopulation and proliferation in the dentate gyrus

The hilus was repopulated with GFAP-overexpressing processes and cells 10 days after pilocarpine-induced SE. Interestingly, when astrocytes were counted at that time, only 14.3 ± 1.7 GFAP-positive cells ($n = 4$) were found within the hilus per section (Fig. 1D, pink arrows, Fig. 2B squares), but many cells in the SGZ (20.1 ± 2.1 cells; $n = 4$) had GFAP-positive processes extending into the hilus (Fig. 1D, pink arrowheads; Fig. 2C). In control mice, only a few subgranular cells with thick, long hilar GFAP-positive processes were found. It is possible that these cells are generated specifically to repopulate the hilus with astrocyte processes after hilar astrocyte loss.

Next, we used BrdU injections and confocal microscopy to examine whether local proliferation contributes to astrocyte repopulation. We compared proliferation within the hilus and the neighboring SGZ (Figs. 5–8), which is well known for cell proliferation during development and after seizures (e.g., Parent et al., 1997; Huttmann et al., 2003). In control mice sacrificed 5 h after the injection of the thymidine analog BrdU, very few BrdU-labeled cells were found in the hilus and the SGZ (Fig. 6). When mice were injected 3 days after SE and analyzed 5 h later, however, the number of BrdU-positive cells was significantly increased in the hilus and there was a trend for an increase in the SGZ (Figs. 5A–E, 6). Of the BrdU-labeled cells in the SGZ, most cells were associated with GFAP-positive processes (Figs. 5A–C, 6C, closed circles). There were at least two different types of subgranular BrdU/GFAP-colabeled cells. One cell type was characterized by a nucleus that was horizontally oriented to the granule cell layer and thick GFAP-positive processes extending into the hilus (Fig. 5A), suggesting that it represents a subgranular proliferating astrocyte. The second type of cell showed a nucleus positioned vertically to the granule cell layer and one process that was radially extended into the granule cell layer (Figs. 5B, C), similar to radial glia which also showed increased proliferation after kainate-induced SE (Huttmann et al., 2003). Some of these radially oriented cells also extended their main process into the hilus, where it appeared to form vascular endfeet (Fig. 5B), similar to the type I cells characterized as astrocytes by Filippov et al. (2003). Three days after SE, 35–52% of the hilar BrdU-positive cells were GFAP-positive (Figs. 5E, 6B), suggesting that astrocyte proliferation or DNA repair occurs in the hilus. To investigate whether cells that were proliferating at 3 days differentiated into

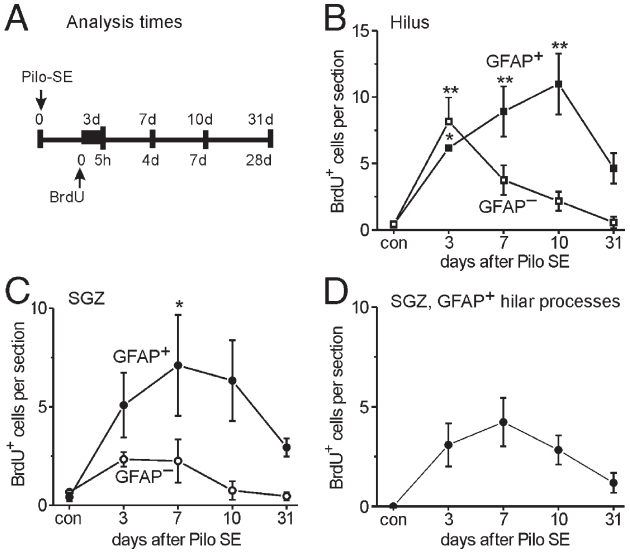

Fig. 6. Time course of proliferation and generation of GFAP-positive cells in the hilus and SGZ after pilocarpine-induced SE in CF1 mice. Panel A illustrates the experimental setup with BrdU injection at 3 days after SE and the times when mice were killed for confocal analysis of BrdU/GFAP fluorescent double-stainings. (B–D) The average number (±SEM) of BrdU-positive cells per eight μm section is shown at different times after SE ($n = 3$–4 mice). Control mice (con) had received saline instead of pilocarpine. BrdU-positive cells associated with (closed symbols) or without (open symbols) GFAP immunoreactivity in their cell body and/or their processes were counted in the hilus (B) and the SGZ (C). Panel B shows that the number of hilar BrdU/GFAP-coexpressing cells increased significantly relatively to control 3 to 10 days after SE, indicating that hilar astrocytes are proliferating after SE. There was a trend for a decrease in the number of double-labeled cells from 10 to 31 days and BrdU labeling was faint at late time points, consistent with dilution of the BrdU label following multiple cell divisions. The number of BrdU-positive, GFAP-negative cells peaked at 3 days after SE and declined thereafter. This is consistent with the majority of these cells being microglial cells, which rapidly divide and invade the injured the hilus 3 days after SE (see Fig. 7B). (C) Subgranular BrdU/GFAP-coexpressing cells increased in numbers up to 7 days after SE, indicating proliferation of subgranular astrocytes, radial glia, and/or potentially neural stem cells. Fewer BrdU-positive cells are GFAP-negative, suggesting proliferation of GFAP-negative neural precursor cells, microglial or endothelial cells and at later times generation of neurons. (D) The subpopulation of subgranular zone BrdU/GFAP-positive cells with GFAP-expressing processes that extend into the hilus, but not the granule cell layer are shown. These cells newly appear after SE, consistent with new subgranular reactive astrocytes being generated, which continue to proliferate in the SGZ subsequent to injury. Lower cell numbers 31 days after SE may be explained by dilution of BrdU during cell division. All statistical comparisons were performed using one-way ANOVAs followed by a Dunnett's multiple comparison test relative to control mice. $^*P < 0.05$, $^{**}P < 0.01$.

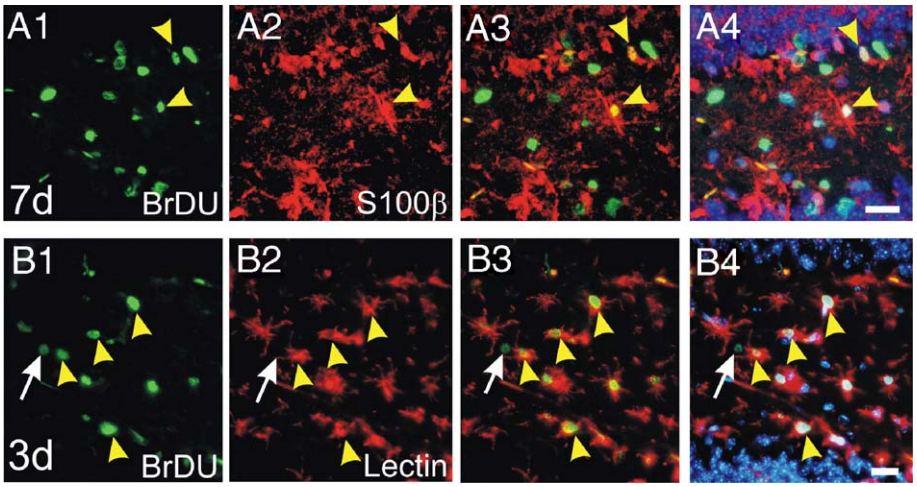

Fig. 7. After pilocarpine-induced SE BrdU/S100β-colabeled mature astrocytes and microglia are found in the hilus of CF1 mice. Mice were injected with BrdU 3 days after SE. Panels A and B illustrate fluorescent double-labelings as indicated in the right hand corner for BrdU (green), S100β (A, red) or *Griffonia simplicifolia* isolectin B_4 (B, red) 4 days after BrdU and 7 days after SE (A), or 5 h after BrdU injection (3 days after SE, B). Panels A1, A2, B1 and B2 show the double-stainings viewed through the green and red filter only. The overlays of the red and green filters (A3, B3) and the Hoechst 33258 counterstain (blue, A4, B4) are shown. Seven days after SE, some BrdU/S100β-colabeled cells were found in the hilus and the SGZ (A, yellow arrowheads), indicating that S100β-positive astrocytes were generated by proliferation. Note that many BrdU-positive cells are colabeled with lectin 3 days after SE, consistent with proliferating microglia (B, yellow arrowheads). The white arrow in panel B points to a BrdU-positive, lectin-negative cell which may represent a proliferating astrocyte or another non-microglial cell type. Scale bars are 20 μm. (For interpretation of the references to colour in this figure legend, the reader is referred to the web version of this article.)

mature astrocytes, mice were killed and analyzed 4, 7 and 28 days after the BrdU injection, corresponding to 7, 10 and 31 days after SE. At 7 and 10 days after SE, the number of BrdU/GFAP double-stained cells increased slightly within the hilus (Figs. 5F, arrowheads; 6B), and hilar BrdU/GFAP-costained cells were still present 31 days after SE (Fig. 5G, arrowheads). Moreover, the number of subgranular GFAP/BrdU-costained cells was increased significantly at 7 days (Fig. 6C, $P < 0.05$; 65% of all BrdU-labeled subgranular cells), and cells persisted up to 31 days after SE (Fig. 5G, arrow). These data indicate that proliferation contributes to the generation of subgranular and hilar GFAP-positive cells.

Fig. 6D depicts the number of subgranular BrdU-positive cell subpopulation with main GFAP-positive processes projecting into the hilus (Figs. 5A, G arrow). The observation that the number of BrdU/GFAP-costained cells increases over several

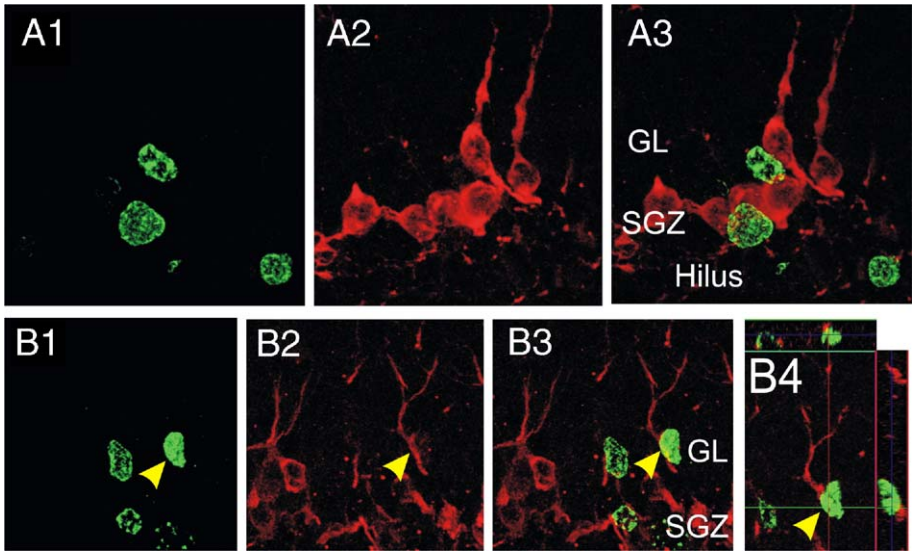

Fig. 8. Neurogenesis after pilocarpine-induced SE in CF1 mice. Confocal analysis of fluorescent BrdU (green) and doublecortin (DCX, red) costainings in mice injected with BrdU 3 days after SE and killed 4 days later, i.e., 7 days after SE. The projections of z-stack images for BrdU (A1, B1), doublecortin (A2, B2) or both (A3, B3) and an orthogonal view (B4) are shown. The majority of BrdU-positive nuclei 7 days after SE were not surrounded by doublecortin-positive cytoplasm (A1–A3), but some colabeled cells were found (B). The yellow arrowhead marks one cell with doublecortin-positive radial processes and the nucleus is at least partially surrounded with doublecortin-expressing cytoplasm, indicating that neurogenesis occurs in this model. GL, granule cell layer; SGZ, subgranular zone. The scale bars represent 20 μm. (For interpretation of the references to colour in this figure legend, the reader is referred to the web version of this article.)

days after a single BrdU injection (Figs. 6B, C) provides further evidence that astrocyte proliferation is ongoing over at least the first 10 days after SE. At later times, especially at 10 and 31 days, the fluorescent BrdU signal was fainter in many cells, consistent with a dilution of BrdU in dividing cells. The relatively low number of BrdU-positive cells at 31 days after SE (Figs. 6B–D) may be explained by the dilution of the BrdU signal below detection threshold or by potential loss of the newly derived cells. At all time points, a large number of BrdU/GFAP-double-stained cells was also found in the dentate molecular layer (not shown), signifying that astrocyte proliferation contributes to gliosis in several areas of the dentate gyrus. Moreover, BrdU/GFAP costained cells were found in other parts of the brain, most notably within the cortex, amygdala, thalamus, the hippocampal stratum lacunosum moleculare and near the pia in CA1 and CA3 areas, indicating that astrocyte proliferation may contribute to gliosis.

In the SGZ, GFAP is expressed not only by astrocytes but also by neural precursor cells that can differentiate into neurons (e.g., Garcia et al., 2004; Seri et al., 2004). To investigate whether the SGZ produced mature astrocytes in this model, we also performed fluorescent double-immunohistochemistry for BrdU and S100β (Fig. 7A), a marker for mature astrocytes in the dentate gyrus (Kligman and Hilt, 1988; Steiner et al., 2004). Indeed, 7 days after SE a sizeable fraction of BrdU-labeled cells was clearly associated with S100β-positive nuclei and processes in the hilus (14%) and in the SGZ (20%; Fig. 7A yellow arrowheads). This indicates that some new hilar and subgranular astrocytes were derived from cells that were dividing 3 days after SE.

About half of the BrdU-positive cells in the hilus were GFAP-negative 3 days after SE (Fig. 6B). At this time, many hilar BrdU-positive cells expressed *G. simplicifolia* isolectin B_4, indicating that many proliferating hilar cells 3 days after SE are microglia ($n = 4$, Fig. 7B, yellow arrowheads). The number of BrdU-positive/GFAP-negative cells declined after 3 days of SE (Fig. 6B), consistent with fast turnover and proliferation of microglia. We have previously shown that 3 days after pilocarpine-induced SE the hilus contains many β2-microglobulin-positive cells with the morphology of microglia (Borges et al., 2003a).

As neurogenesis is prominent in other seizure models, we next investigated whether subgranular neurogenesis occurs in the pilocarpine mouse model 7 days after SE. Using fluorescent and confocal analysis of sections double-stained for BrdU and the immature neuronal marker doublecortin (Rao and Shetty, 2004), we found mainly doublecortin-negative/BrdU-positive cells in the SGZ and granule cell layer (Fig. 8A, white arrowheads). However, we also observed several BrdU-labeled nuclei that were surrounded by the immature neuronal marker doublecortin (Fig. 8B, yellow arrowheads; $n = 4$ mice), indicating that neurogenesis occurs in this model in parallel to astrogenesis.

Discussion

Using light and electron microscopy we show here that astrocytes in the mouse dentate hilus degenerate soon after pilocarpine-induced SE in different mouse strains. One week after SE, the hilus is repopulated by astrocytes and astrocyte processes emanating from cells located in the SGZ. These astrocytes were produced at least partially by local proliferation in the hilus and the SGZ.

Selective vulnerability of hilar astrocytes

A major finding of this study is that hilar GFAP labeling was lost after pilocarpine-induced SE in mice. This finding was very reproducible and was observed in several mouse strains, including CF1, two 129 substrains and C57BL/6CR mice (data not shown), but not in rat or after kainate-induced SE in the mouse. Astrocyte degeneration at the light microscopic level in paraffin sections was confirmed by electron microscopy, showing degenerated astrocytic processes and somata of glial cells (Fig. 3C). The relatively small cell diameter of the degenerating cells makes us confident that the degenerating somata are glial. Although the phenotype of degenerated cell bodies may be hard to characterize, the presence of degenerated astrocytic processes (Fig. 3A) throughout the neuropil combined with the loss of GFAP-containing elements provide correlative evidence to support the existence of degenerated astrocyte cell bodies in the dentate gyrus. To our knowledge, astrocyte degeneration has not been reported before in the hilus. However, transient loss of GFAP immunoreactivity (Jorgensen et al., 1993) and swelling of astrocytes (Nadler et al., 1980; Nitecka et al., 1984) have been reported within the mossy fiber pathway and CA3 pyramidal cell layer after kainate injection in rats, and we have observed loss of GFAP expression in the piriform cortex of pilocarpine-treated rats (Borges et al., 2003b). Astrocyte degeneration in the hilus was not observed after kainate-induced SE, possibly due to less severe SE in the kainate than pilocarpine mouse model. Hilar neuron degeneration occurred as early as 6 h after pilocarpine-induced SE (Borges et al., 2003a), before any obvious changes in hilar GFAP expression. Therefore, loss of hilar astrocytes is unlikely to induce hilar neuron death. However, we cannot rule out the possibility that early impairment of hilar astrocyte function, such as uptake of potassium and glutamate, may contribute to neuronal death and/or seizure generation. It would be of interest to determine whether astrocytes are also injured in human temporal lobe epilepsy (TLE) with hippocampal sclerosis.

Why do hilar but not molecular layer astrocytes degenerate after pilocarpine-induced SE in the mouse dentate gyrus? First, it is possible that hilar astrocytes are simply overwhelmed by the *extensive* local neurodegeneration that occurs in the dentate hilus in this epilepsy model, perhaps reacting to imbalanced ion and neurotransmitter concentrations or spillage of cytoplasm from dying neurons. This is consistent with several correlations observed. We found no evidence of astrocyte loss in the molecular layer, which lacks neuronal degeneration, and we observed no hilar astrocyte loss in the kainate model, in which hilar neurons remained intact (see also Schauwecker and Steward, 1997). In rats, no signs of GFAP loss or astrocyte damage were observed after SE induced by pilocarpine, which may be explained by the finding that many hilar neurons were still intact. In contrast, we found permanent astrocyte damage after lithium/pilocarpine-induced SE in the rat piriform cortex, which shows frank loss of neurons (Borges et al., 2003b). Alternatively, hilar astrocytes may

be intrinsically more vulnerable to damage than astrocytes in the nearby dentate molecular layer. For example, many hilar astrocytes, in contrast to molecular layer astrocytes, contain Gomori-positive inclusions (Ohm et al., 1992), which originate from transformed mitochondria that become engulfed in lysosomes and contain peroxidase activity, heme, copper and reactive SH groups (Schipper, 1991). These inclusions may be an indicator of chronic oxidative stress (Schipper, 1996), but the cause and role of the inclusions in brain pathology remains largely unclear.

Partial astrocyte repopulation by proliferation

Another important question is how astrocytes reappear in the mouse hilus within a week of SE-induced degeneration. In untreated mice, astrogenesis occurs within the SGZ (Eckenhoff and Rakic, 1988; Steiner et al., 2004) and within the hilus (Bondolfi et al., 2004). Moreover, after ischemia many BrdU/GFAP-double-labeled cells were found within the hilus (Sharp et al., 2002). Consistent with these studies, we found BrdU/GFAP-double-labeled cells within the hilus and within the SGZ 5 h after BrdU injection. Moreover, there was a trend toward increasing numbers of BrdU/GFAP-positive cells up to 7 days after BrdU injection. These data indicate that in the pilocarpine mouse model GFAP-positive cells proliferate in both the hilus and the SGZ. Many BrdU-containing cell bodies were found within or close to the SGZ and their main GFAP-overexpressing processes extended into the hilus. These cells appear to be newly generated, potentially reactive astrocytes, as neural stem cells with this morphology have not been described. Surviving hilar astrocytes, subgranular astrocytes as well as stem cells are likely to proliferate in response to the pilocarpine-induced seizures and/or hilar injury. Our data demonstrate that the subgranular zone is not only a zone of neurogenesis after seizures but also astrogenesis.

Our findings in the pilocarpine mouse model appear to differ from other seizure models, in which predominant neurogenesis but little astrogenesis was found in the dentate gyrus (e.g., Parent et al., 1997; Scott et al., 2000; Ferland et al., 2002). Differences in the timing of BrdU injection and tissue analysis are likely to contribute to this apparent discrepancy. In our studies, BrdU was injected early after SE, and tissue was harvested as early as 5 h after injection, whereas most experiments in the mentioned reports used much longer post-BrdU harvest times, for which the BrdU label is expected to be diluted out of many dividing astrocytes. It is possible that astrogenesis is more pronounced early after seizures. Although we observed pronounced astrogenesis, we also found BrdU/doublecortin-labeled immature neurons 7 days after SE, indicating that neurogenesis also occurs in the pilocarpine mouse model. A more careful study with BrdU injections and analysis of multiple neuronal markers at various time points would be needed to compare the extent of astrogenesis and neurogenesis in epilepsy models.

Functional implications

In healthy brains, astrocyte somata are evenly spaced and only the tips of astrocyte processes overlap (Bushong et al., 2002; Ogata and Kosaka, 2002). However, an uneven GFAP distribution was obvious in the gliotic hilus as late as 31 days after pilocarpine-induced SE (Fig. 1D). Whether the disorganization of astrocytes produces functional disturbances remains to be determined. Moreover, the presence of subgranular astrocytes with hilar processes may point to earlier astrocyte damage, as these cells were only found in the pilocarpine, but not kainate mouse model. Therefore, it is possible that even at late stages the morphology and distribution of astrocytes may indicate astrocyte damage in other brain disorders and brain areas.

What are the functional consequences of astrocyte degeneration and subsequent partial repopulation of the mouse dentate hilus, and the potential implications for epileptogenesis? Interestingly, the extent of both astrocyte and neuron degeneration in the hilus correlated with our ability to detect spontaneous seizures in CF1mice. Eleven to seventeen days after pilocarpine-induced SE, we observed spontaneous seizures (Borges et al., 2003a), but we did not find any spontaneous seizures up to 35 days after kainate-induced SE (Borges et al., 2004). The possibility remains that spontaneous seizures are rare in the kainate CF1 mouse model or that they develop late (e.g., Lahteinen et al., 2002). By contrast, pilocarpine or lithium/pilocarpine-induced SE in the rat leads to spontaneous seizures accompanied by severe neuronal and astroglial degeneration in the piriform cortex but not dentate hilus.

Astrocytes play important roles in regulating neuronal excitability, for example, by controlling the extracellular concentrations of potassium, glutamate and adenosine. Indeed, paroxysmal depolarization shifts can be caused by photolysis of caged calcium in astrocytes and glutamate release from an extrasynaptic source, presumably astrocytes (Tian et al., 2005). On the other hand, a low concentration of fluorocitrate, which is thought to inhibit selectively astroglial metabolism by inhibiting aconitase, an enzyme integral to the tricarboxylic acid cycle (Paulsen et al., 1987), can evoke focal seizures (Willoughby et al., 2003). Loss of astrocytes or altered astrocyte function in the hilus is likely to alter neuronal signaling in the dentate gyrus. The dentate gyrus controls input into the CA3 and CA1 area and is highly sensitive to changes in extracellular potassium (reviewed by Nadler, 2003), especially in TLE patients with hippocampal sclerosis (Gabriel et al., 2004). Whether repopulating hilar astrocytes have properties that contribute to hyperexcitability and epileptogenesis in animal epilepsy models (e.g., Gouder et al., 2004) is an interesting issue for future work. Pro-convulsive astrocyte properties have been found in human TLE tissue (e.g., Hinterkeuser et al., 2000; Bordey and Spencer, 2004; Eid et al., 2004). In surgically resected tissue from TLE patients with hippocampal sclerosis, hilar astrocytes display smaller inwardly rectifying potassium currents (Bordey and Spencer, 2004), and the dentate is more sensitive to elevated potassium compared to tissue without sclerosis (Gabriel et al., 2004). These findings suggest that potassium buffering by hilar astrocytes may be impaired in human epileptic hippocampi.

In conclusion, this study shows SE-induced hilar astrocyte degeneration and subsequent astrocyte repopulation, in part by local proliferation. Our data together with findings from other epilepsy models and human TLE tissue raise further interest in a potential role of astrocytes in seizure generation and epileptogenesis. Insight into the functional consequences of astrocyte heterogeneity, astrocyte loss and astrogenesis may lead to a better

understanding of the role of astrocytes in brain injury and epilepsy and potential new therapeutic strategies.

Acknowledgments

We are grateful to Lucy Liaw and Susan Rittling for sending us 129 mice, Walt Hubert and Marc Verreault for preparing the tissue for electron microscopy and Frank Gordon for statistical advice. The authors thank Robert Baul, Marla Gearing and Veronica Walker for help with paraffin sections and immunostainings.

References

Bengzon, J., Kokaia, Z., Elmer, E., Nanobashvili, A., Kokaia, M., Lindvall, O., 1997. Apoptosis and proliferation of dentate gyrus neurons after single and intermittent limbic seizures. Proc. Natl. Acad. Sci. U. S. A. 94, 10432–10437.

Bondolfi, L., Ermini, F., Long, J.M., Ingram, D.K., Jucker, M., 2004. Impact of age and caloric restriction on neurogenesis in the dentate gyrus of C57BL/6 mice. Neurobiol. Aging 25, 333–340.

Bordey, A., Spencer, D.D., 2004. Distinct electrophysiological alterations in dentate gyrus versus CA1 glial cells from epileptic humans with temporal lobe sclerosis. Epilepsy Res. 59, 107–122.

Borges, K., Gearing, M., McDermott, D.L., Smith, A.B., Almonte, A.G., Wainer, B.H., Dingledine, R., 2003a. Neuronal and glial pathological changes during epileptogenesis in the mouse pilocarpine model. Exp. Neurol. 182, 21–34.

Borges, K., Irier, H., McDermott, D., Hubert, W., Smith, Y., Dingledine, R., 2003b. Region-specific astrocyte degeneration after pilocarpine-induced status epilepticus. Abstr. Soc. Neurosci. 33rd Ann. Meeting, No. 378.16.

Borges, K., McDermott, D.L., Dingledine, R., 2004. Reciprocal changes of CD44 and GAP-43 expression in the dentate gyrus inner molecular layer after status epilepticus in mice. Exp. Neurol. 188, 1–10.

Bushong, E.A., Martone, M.E., Jones, Y.Z., Ellisman, M.H., 2002. Protoplasmic astrocytes in CA1 stratum radiatum occupy separate anatomical domains. J. Neurosci. 22, 183–192.

Clifford, D.B., Olney, J.W., Maniotis, A., Collins, R.C., Zorumski, C.F., 1987. The functional anatomy and pathology of lithium-pilocarpine and high-dose pilocarpine seizures. Neuroscience 23, 953–968.

Eckenhoff, M.F., Rakic, P., 1988. Nature and fate of proliferative cells in the hippocampal dentate gyrus during the life span of the rhesus monkey. J. Neurosci. 8, 2729–2747.

Eid, T., Thomas, M.J., Spencer, D.D., Runden-Pran, E., Lai, J.C., Malthankar, G.V., Kim, J.H., Danbolt, N.C., Ottersen, O.P., de Lanerolle, N.C., 2004. Loss of glutamine synthetase in the human epileptogenic hippocampus: possible mechanism for raised extracellular glutamate in mesial temporal lobe epilepsy. Lancet 363, 28–37.

Eng, L.F., Yu, A.C., Lee, Y.L., 1992. Astrocytic response to injury. Prog. Brain Res. 94, 353–365.

Ferland, R.J., Gross, R.A., Applegate, C.D., 2002. Increased mitotic activity in the dentate gyrus of the hippocampus of adult C57BL/6J mice exposed to the flurothyl kindling model of epileptogenesis. Neuroscience 115, 669–683.

Filippov, V., Kronenberg, G., Pivneva, T., Reuter, K., Steiner, B., Wang, L.P., Yamaguchi, M., Kettenmann, H., Kempermann, G., 2003. Subpopulation of nestin-expressing progenitor cells in the adult murine hippocampus shows electrophysiological and morphological characteristics of astrocytes. Mol. Cell. Neurosci. 23, 373–382.

Gabriel, S., Njunting, M., Pomper, J.K., Merschhemke, M., Sanabria, E.R., Eilers, A., Kivi, A., Zeller, M., Meencke, H.J., Cavalheiro, E.A., Heinemann, U., Lehmann, T.N., 2004. Stimulus and potassium-induced epileptiform activity in the human dentate gyrus from patients with and without hippocampal sclerosis. J. Neurosci. 24, 10416–10430.

Gage, F.H., Kempermann, G., Palmer, T.D., Peterson, D.A., Ray, J., 1998. Multipotent progenitor cells in the adult dentate gyrus. J. Neurobiol. 36, 249–266.

Garcia, A.D., Doan, N.B., Imura, T., Bush, T.G., Sofroniew, M.V., 2004. GFAP-expressing progenitors are the principal source of constitutive neurogenesis in adult mouse forebrain. Nat. Neurosci. 7, 1233–1241.

Gouder, N., Scheurer, L., Fritschy, J.M., Boison, D., 2004. Overexpression of adenosine kinase in epileptic hippocampus contributes to epileptogenesis. J. Neurosci. 24, 692–701.

Gurnett, C.A., Landt, M., Wong, M., 2003. Analysis of cerebrospinal fluid glial fibrillary acidic protein after seizures in children. Epilepsia 44, 1455–1458.

Hinterkeuser, S., Schroder, W., Hager, G., Seifert, G., Blumcke, I., Elger, C.E., Schramm, J., Steinhauser, C., 2000. Astrocytes in the hippocampus of patients with temporal lobe epilepsy display changes in potassium conductances. Eur. J. Neurosci. 12, 2087–2096.

Hof, P., Young, W.G., Bloom, F.E., Belichenko, P.V., Celio, M.R., 2000. Comparative Cytoarchitonic Atlas of the C57BL/6 and 129/Sv Mouse Brains. Elsevier, New York.

Huttmann, K., Sadgrove, M., Wallraff, A., Hinterkeuser, S., Kirchhoff, F., Steinhauser, C., Gray, W.P., 2003. Seizures preferentially stimulate proliferation of radial glia-like astrocytes in the adult dentate gyrus: functional and immunocytochemical analysis. Eur. J. Neurosci. 18, 2769–2778.

Jorgensen, M.B., Finsen, B.R., Jensen, M.B., Castellano, B., Diemer, N.H., Zimmer, J., 1993. Microglial and astroglial reactions to ischemic and kainic acid-induced lesions of the adult rat hippocampus. Exp. Neurol. 120, 70–88.

Kempermann, G., Gage, F.H., 2002. Genetic influence on phenotypic differentiation in adult hippocampal neurogenesis. Brain Res. Dev. Brain Res. 134, 1–12.

Kempermann, G., Jessberger, S., Steiner, B., Kronenberg, G., 2004. Milestones of neuronal development in the adult hippocampus. Trends Neurosci. 27, 447–452.

Kettenmann, H., Ransom, B.R., 2004. Neuroglia, 2nd ed. Oxford University Press, Oxford, UK.

Kligman, D., Hilt, D.C., 1988. The S100 protein family. Trends Biochem. Sci. 13, 437–443.

Krum, J.M., 1994. Experimental gliopathy in the adult rat CNS: effect on the blood-spinal cord barrier. Glia 11, 354–366.

Lahteinen, S., Pitkanen, A., Saarelainen, T., Nissinen, J., Koponen, E., Castren, E., 2002. Decreased BDNF signalling in transgenic mice reduces epileptogenesis. Eur. J. Neurosci. 15, 721–734.

Liaw, L., Birk, D.E., Ballas, C.B., Whitsitt, J.S., Davidson, J.M., Hogan, B.L., 1998. Altered wound healing in mice lacking a functional osteopontin gene (spp1). J. Clin. Invest. 101, 1468–1478.

Lie, D.C., Song, H., Colamarino, S.A., Ming, G.L., Gage, F.H., 2004. Neurogenesis in the adult brain: new strategies for central nervous system diseases. Annu. Rev. Pharmacol. Toxicol. 44, 399–421.

Motte, J., Fernandes, M.J., Baram, T.Z., Nehlig, A., 1998. Spatial and temporal evolution of neuronal activation, stress and injury in lithium-pilocarpine seizures in adult rats. Brain Res. 793, 61–72.

Nadler, J.V., 2003. The recurrent mossy fiber pathway of the epileptic brain. Neurochem. Res. 28, 1649–1658.

Nadler, J.V., Perry, B.W., Gentry, C., Cotman, C.W., 1980. Degeneration of hippocampal CA3 pyramidal cells induced by intraventricular kainic acid. J. Comp. Neurol. 192, 333–359.

Newman, E.A., 2003. New roles for astrocytes: regulation of synaptic transmission. Trends Neurosci. 26, 536–542.

Niquet, J., Ben-Ari, Y., Represa, A., 1994. Glial reaction after seizure induced hippocampal lesion: immunohistochemical characterization of proliferating glial cells. J. Neurocytol. 23, 641–656.

Nitecka, L., Tremblay, E., Charton, G., Bouillot, J.P., Berger, M.L., Ben-Ari, Y., 1984. Maturation of kainic acid seizure-brain damage syndrome in the rat: II. Histopathological sequelae. Neuroscience 13, 1073–1094.

Ogata, K., Kosaka, T., 2002. Structural and quantitative analysis of astrocytes in the mouse hippocampus. Neuroscience 113, 221–233.

Ohm, T.G., Jung, E., Schnecko, A., 1992. A subpopulation of hippocampal glial cells specific for the zinc-containing mossy fibre zone in man. Neurosci. Lett. 145, 181–184.

Palmer, T.D., Willhoite, A.R., Gage, F.H., 2000. Vascular niche for adult hippocampal neurogenesis. J. Comp. Neurol. 425, 479–494.

Parent, J.M., 2003. Injury-induced neurogenesis in the adult mammalian brain. Neuroscientist 9, 261–272.

Parent, J.M., Yu, T.W., Leibowitz, R.T., Geschwind, D.H., Sloviter, R.S., Lowenstein, D.H., 1997. Dentate granule cell neurogenesis is increased by seizures and contributes to aberrant network reorganization in the adult rat hippocampus. J. Neurosci. 17, 3727–3738.

Paulsen, R.E., Contestabile, A., Villani, L., Fonnum, F., 1987. An in vivo model for studying function of brain tissue temporarily devoid of glial cell metabolism: the use of fluorocitrate. J. Neurochem. 48, 1377–1385.

Peters, A., Palay, S.L., Webster, H., 1991. The Fine Structure of the Nervous System: Neurons and their Supporting Cells, 3rd ed. Oxford University Press, Oxford. 494 pp.

Petito, C.K., Olarte, J.P., Roberts, B., Nowak Jr., T.S., Pulsinelli, W.A., 1998. Selective glial vulnerability following transient global ischemia in rat brain. J. Neuropathol. Exp. Neurol. 57, 231–238.

Rao, M.S., Shetty, A.K., 2004. Efficacy of doublecortin as a marker to analyse the absolute number and dendritic growth of newly generated neurons in the adult dentate gyrus. Eur. J. Neurosci. 19, 234–246.

Revuelta, M., Castano, A., Machado, A., Cano, J., Venero, J.L., 2005. Kainate-induced zinc translocation from presynaptic terminals causes neuronal and astroglial cell death and mRNA loss of BDNF receptors in the hippocampal formation and amygdala. J. Neurosci. Res. 82, 184–195.

Rittling, S.R., Matsumoto, H.N., McKee, M.D., Nanci, A., An, X.R., Novick, K.E., Kowalski, A.J., Noda, M., Denhardt, D.T., 1998. Mice lacking osteopontin show normal development and bone structure but display altered osteoclast formation in vitro. J. Bone Miner. Res. 13, 1101–1111.

Schauwecker, P.E., Steward, O., 1997. Genetic determinants of susceptibility to excitotoxic cell death: implications for gene targeting approaches. Proc. Natl. Acad. Sci. U. S. A. 94, 4103–4108.

Schipper, H.M., 1991. Gomori-positive astrocytes: biological properties and implications for neurologic and neuroendocrine disorders. Glia 4, 365–377.

Schipper, H.M., 1996. Astrocytes, brain aging, and neurodegeneration. Neurobiol. Aging 17, 467–480.

Scott, B.W., Wojtowicz, J.M., Burnham, W.M., 2000. Neurogenesis in the dentate gyrus of the rat following electroconvulsive shock seizures. Exp. Neurol. 165, 231–236.

Seri, B., Garcia-Verdugo, J.M., McEwen, B.S., Alvarez-Buylla, A., 2001. Astrocytes give rise to new neurons in the adult mammalian hippocampus. J. Neurosci. 21, 7153–7160.

Seri, B., Garcia-Verdugo, J.M., Collado-Morente, L., McEwen, B.S., Alvarez-Buylla, A., 2004. Cell types, lineage, and architecture of the germinal zone in the adult dentate gyrus. J. Comp. Neurol. 478, 359–378.

Sharp, F.R., Liu, J., Bernabeu, R., 2002. Neurogenesis following brain ischemia. Brain Res. Dev. Brain Res. 134, 23–30.

Steiner, B., Kronenberg, G., Jessberger, S., Brandt, M.D., Reuter, K., Kempermann, G., 2004. Differential regulation of gliogenesis in the context of adult hippocampal neurogenesis in mice. Glia 46, 41–52.

Thomas, L.B., Gates, D.J., Richfield, E.K., O'Brien, T.F., Schweitzer, J.B., Steindler, D.A., 1995. DNA end labeling (TUNEL) in Huntington's disease and other neuropathological conditions. Exp. Neurol. 133, 265–272.

Tian, G.F., Azmi, H., Takano, T., Xu, Q., Peng, W., Lin, J., Oberheim, N., Lou, N., Wang, X., Zielke, H.R., Kang, J., Nedergaard, M., 2005. An astrocytic basis of epilepsy. Nat. Med. 11, 973–981.

Willis, C.L., Nolan, C.C., Reith, S.N., Lister, T., Prior, M.J., Guerin, C.J., Mavroudis, G., Ray, D.E., 2004. Focal astrocyte loss is followed by microvascular damage, with subsequent repair of the blood–brain barrier in the apparent absence of direct astrocytic contact. Glia 45, 325–337.

Willoughby, J.O., Mackenzie, L., Broberg, M., Thoren, A.E., Medvedev, A., Sims, N.R., Nilsson, M., 2003. Fluorocitrate-mediated astroglial dysfunction causes seizures. J. Neurosci. Res. 74, 160–166.